

# Estimate of the rate of collisional-radiative recombination of doubly charged $\text{Ne}^{++}$ ions from the results of a spectroscopic experiment

© V.A. Ivanov

St. Petersburg State University, St. Petersburg, Russia

e-mail: v.a.ivanov@spbu.ru

Received June 28, 2023

Revised June 28, 2023

Accepted Oct 16, 2023

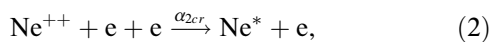
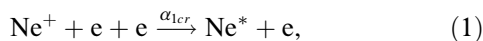
An experiment was set up to study the afterglow of an extended barrier discharge in low-pressure neon containing  $\text{Ne}^+$ ,  $\text{Ne}^{2+}$ , and  $\text{Ne}^{++}$  ions by kinetic spectroscopy. Observation conditions: neon pressure  $\sim 0.8\text{--}1.7$  Torr, electron density in the afterglow stage  $[e] \sim 10^{11} \text{ cm}^{-3}$ . In order to compare the rates of collisional-radiative recombination of  $\text{Ne}^+$  and  $\text{Ne}^{++}$  ions, the effect of pulsed „heating“ of decaying plasma electrons by a weak high-frequency field on the intensities of atomic and ion lines was observed. The presented data show that in such a plasma, short-term suppression of recombination processes by electron heating leads to an increase in the brightness of spectral lines in the atomic and ion afterglow spectra, and the reaction of the lines of the latter turns out to be much stronger. Based on simple estimates, it is shown that this effect is due to the difference in the recombination rates of the  $\text{Ne}^+$  and  $\text{Ne}^{++}$  ions, and this difference turns out to be beyond the scope of theoretical concepts.

**Keywords:** dielectric barrier discharge, doubly charged ions, collisional-radiative recombination, decaying plasma, elementary processes.

DOI: 10.61011/EOS.2023.11.58042.5370-23

## Introduction

This work is a continuation of the study of collisional radiative recombination (CRR) of doubly charged neon ions, first discovered in the afterglow of a barrier discharge in the work [1]. In [2,3], on the basis of a comparison of spectroscopic observations of the atomic and ionic spectral lines emission with model calculations, a conclusion on a much more radical difference in the rates of CRR processes was made



where  $\alpha_{1cr}$  and  $\alpha_{2cr}$  — recombination coefficients than predicted by theory [4] and calculations [5]. This approach — a comparison of experimental data with numerical calculations that take into account the main processes in plasma is a standard procedure for finding the rate constants of the processes under study. However, it has an obvious and difficult to overcome drawback in the case when the model contains a large number of elementary processes, the rate constants of which are known (measured or calculated) with low accuracy — their variation within the specified errors can lead to a scatter in the value of the desired constant, exceeding the standard deviation of the experimental data used. Taking into account the fundamental nature of the processes under consideration and their role in the formation of the properties of low-temperature plasma, in this work we present the results of a spectroscopic experiment that allows us to compare the constants  $\alpha_{1cr}$  and  $\alpha_{2cr}$  without resorting to the mentioned procedure.

The opportunity of obtaining information on the rates of recombination processes from spectroscopic observation data in a decaying plasma is generally speaking not obvious. To implement it, it is required the intensities of the spectral lines to be proportional to the recombination fluxes that determine the loss of the corresponding ions. For processes (1), (2) this relationship is as the following:

$$J_a(t) \sim \alpha_{1cr}[e]^2[\text{Ne}^+] = -d[\text{Ne}^+]/dt, \quad (3)$$

$$J_i(t) \sim \alpha_{2cr}[e]^2[\text{Ne}^{++}] = -d[\text{Ne}^{++}]/dt, \quad (4)$$

Let us briefly recall how the CRR process is reviewed in theoretical models. <sup>1</sup> Historically, the first of them — the Thomson model [6] — predicts the dependence of the probability of electron capture by an ion in a triple collision (1) on plasma parameters. This probability depends on the electron temperature as  $Te^{-4.5}$ , and in this approach, the capture of an electron by an ion in a triple collision represents a single recombination event. In the subsequent models [4,5,7,9] electron-ion recombination is reviewed as a complex kinetic process involving both direct (in the direction of the arrow in reactions (1), (2)), and reverse (ionization) transitions with the need to analyze the distribution of excited atoms over bond energy, taking into account their devastation due to emission transitions. In the limiting case of purely collisional kinetics of highly excited atoms (for them this limit is realized primarily due to a decrease in the probability of radiative transitions with

<sup>1</sup> The CRR mechanism has been reviewed in a large number of studies; here we mention only the main (in our opinion) of them, the results of which are directly related to the conclusions of this work. An exhaustive list of studies is contained in [7,8].

increasing principal quantum number [10]), the authors [4] review CRR as diffusion the excited electron „down“ to the ground state of the atom due to interaction with free electrons of the plasma, while the highly excited states of the atom with the bond energy  $\varepsilon^* \leq T_e$  are in equilibrium with the continuum. The authors [4] found as the recombination coefficient

$$\alpha_{Zcr} = C^* Z^3 [e] \Lambda T_e^{-4.5}, \quad (5)$$

where  $C$  — constant,  $Z$  — ion charge,  $\Lambda = \ln \sqrt{(Z^2 + 1)}$  — Coulomb logarithm for bound states, emphasizing that the result is valid for  $Z \gg 1$ , and for small  $Z$  the application of (5) is justified only in view of the weak (logarithmic) dependence  $\Lambda(Z)$ . Note that when applied to our problem of comparing the recombination rates of ions with charges  $Z = 2$  and  $Z = 1$ , the dependence of  $\Lambda$  on  $Z$  turns out to be very noticeable:  $\Lambda(2)/\Lambda(1) \approx 2.3$ . Taking into account the uncertainty in the value of  $\Lambda(Z)$  in formula (5) [8], we will assume that the dependence of the recombination coefficient on  $Z$  corresponds to  $Z^3$ . Let us note that a formula similar to (5) for the recombination coefficient of singly charged ions was derived in a number of works, a detailed analysis of which is contained in [8].

It is obvious that the intensity of radiation from excited atoms that are in a state close to equilibrium is not described by relations (3), (4). This means that in order to solve the problem posed, the experiment must be carried out under conditions where, on the one hand, the departure of ions in the decaying stage is carried out according to the CRR mechanism (i.e., the electron densities are sufficiently high), on the other hand, for spectroscopic observations, it is required to select levels with a sufficiently high bond energy, the depletion of which occurs primarily due to radiation, which carries the recombination flux. The corresponding criteria are formulated in several works (for example, [7,11]). The assessments based on them show that the lines selected in this work satisfy these criteria. Thus, in the atomic spectrum, the main measurements were carried out on the 576.44 nm line, the upper level  $4d$  of which has the bond energy  $\varepsilon^* = 0.86$  eV, in the ionic spectrum — on the lines 333.48 nm ( $E^* = 30.88$ ,  $\varepsilon^* > 10$  eV) and 439.20 nm (level  $4f$ ,  $\varepsilon^* > 3.5$ ) with electron density  $[e] \sim 10^{11} \text{ cm}^{-3}$  and electron temperature in the afterglow, as assessed based on the model [2] beyond the recombination maximum (see below) less than 500 K. The implementation of this condition is confirmed directly by experimental observations, which are discussed below. With regard to the relationship between the CRR rate under the conditions discussed and in the collisional limit, the answer is easy to find using the recombination coefficient approximation [9]:

$$\alpha = 1.55 \cdot 10^{-10} \cdot T_e^{-0.63} + 6.0 \cdot 10^{-9} \cdot T_e^{-2.18} \cdot [e]^{0.37} + 3.8 \cdot 10^{-9} \cdot T_e^{-4.5} \cdot [e]. \quad (6)$$

Here  $T_e$  — in kelvins,  $[e]$  — in  $\text{cm}^{-3}$ , recombination coefficient  $\alpha$  is related to  $\alpha_{1cr}$  as  $\alpha = \alpha_{1cr}[e]$  and has the dimension  $\text{cm}^3 \text{s}^{-1}$ . The proposed approximation allows

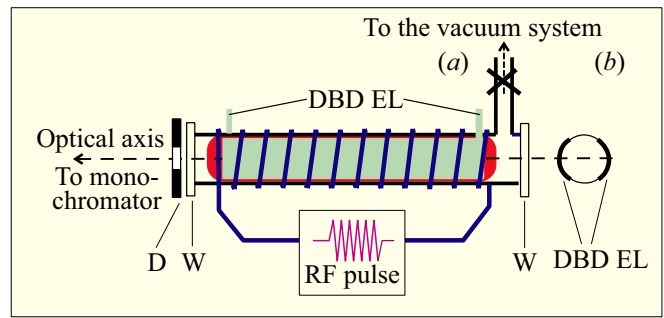


**Figure 1.** (a) Diagram of superposition of barrier discharge and pulsed radio-frequency discharge (RF Pulse),  $D$  — diaphragm 5 mm in diameter;  $W$  — are quartz windows. (b) Positioning of DBD electrodes on the external side surface of a discharge tube.

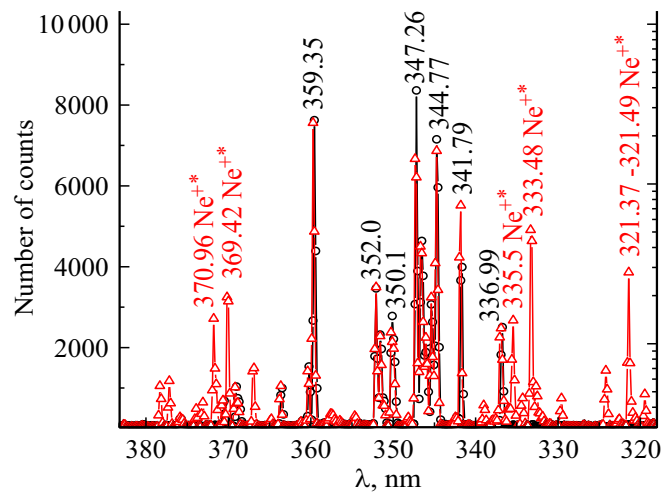


**Figure 2.** Afterglow spectra in the early and late stages. Circles — gate interval  $\Delta t_1$ , triangles —  $\Delta t_2$ . Neon pressure  $P_{\text{Ne}} = 1.7$  Torr.

to trace the change in the recombination coefficient of singly charged ions in a wide range of plasma parameters. Calculations using (6) show that for  $T_e \leq 500$  K and  $[e] \geq 5 \cdot 10^{10}$  the third term is more than twice the sum of the first two.

## 1. Experimental procedure and results

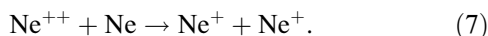
As a plasma source, we used a low-frequency (80–300 Hz) dielectric barrier discharge (DBD) in neon in a cylindrical glass tube 25 cm long and an internal diameter of 3.8 cm (Fig. 1), filled with neon at pressures of about 1 Torr. For a detailed description of the discharge, see [1]. Plasma in such a discharge is created by applying a high-voltage pulse to the electrodes, forming two half-waves of current of opposite polarity, each lasting several microseconds. As the pressure decreases to the indicated values, the spectrum of its radiation becomes enriched with ionic lines [1–3], as shown in Fig. 2 in the near ultraviolet

region, where the effect is most pronounced. It can be seen that the ion spectrum disappears with time in the early afterglow. This observation complements the comparison of the spectra of DBD and a radio frequency discharge that does not excite ion lines [1–3]. In a pulsed mode with an amplitude-controlled radio frequency field strength, we used an RF discharge for short-term „heating“ of electrons at the stage of plasma decay. The electron concentration in the DBD afterglow was assessed from the response of the atomic density Ne(3s(<sup>3</sup>P<sub>1</sub>)) to pulsed heating of electrons [1] and in the afterglow stage used for processing the experimental data it was close to 10<sup>11</sup> cm<sup>-3</sup>.

The data in Fig. 2 were obtained by gating the photomultiplier tube signal (light fluxes were recorded using the photon counting method) at the time intervals shown in Fig. 3. Spectrum corresponding to the  $\Delta t_1$  interval — typical afterglow spectrum of a direct current discharge or RF discharge, repeatedly observed in experiments and formed by competing processes CRR (1) (line 576.4 nm transition 4d → 3p, Fig. 3) and CRR together with dissociative recombination (DR) of molecular ions Ne<sub>2</sub><sup>+</sup> (lines 585.25 nm, 3p → 3s and 344.77 nm, 4p → 3s, Fig. 3). Here it is appropriate to recall the general property characteristic of the DR mechanism of inert gas ions (with the exception of helium), which consists in the presence of a limit on the excitation energy that determines the levels available for population due to DR: these are the levels located in energy at resonance or below the main vibrational level of the molecular ion. In the case of neon, this boundary separates 10 levels of the 2p<sup>5</sup>4p configuration so that only the lower six are associated with the recombination of molecular ions [12]. In a decaying plasma with electron „heating“ this boundary shifts to the region of highly excited states [13].

The flux of quanta in the 576.44 nm line, as can be seen from the data in Fig. 3, not only decreases faster with time in the afterglow compared to the 585.25 nm line, but also has a significantly deeper dip at the beginning of the afterglow, reflecting a radically stronger dependence of the rate of collisional-radiative recombination on electron temperature compared to DR.

The rapid decay of ion lines (Fig. 3) is due to two reasons. Firstly, a significantly higher recombination rate of doubly charged ions (2), and, secondly, the escape of ions due to the process of charge transfer during collisions with atoms:



Regarding the rate constant of this process, the literature contains contradictory data: the [14] suggests  $k_{\text{Ne}} = 9 \cdot 10^{-14}$  cm<sup>3</sup>/s, while according to the data [15]  $k_{\text{Ne}}$  varies within the range (1.9–2.7) · 10<sup>-14</sup> cm<sup>3</sup>/s depending on the state of the ion Ne<sup>++</sup>.

In order to confirm the implementation of the above-mentioned criterion of proportionality of the intensities of spectral lines to recombination fluxes, we recorded the emission of levels with different bond energies of the excited electron. We found no differences in the afterglow

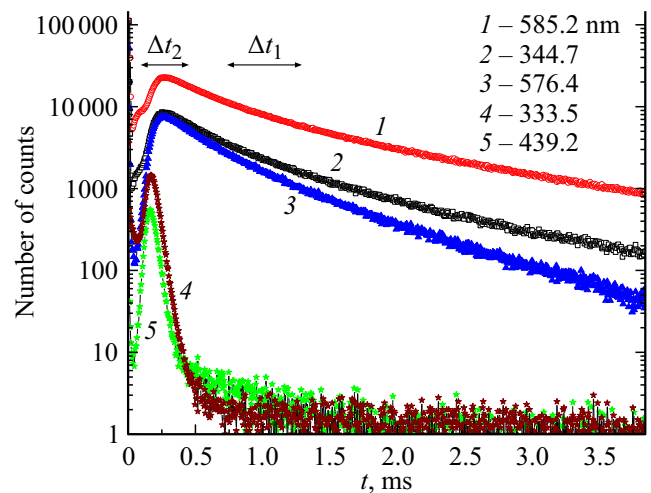


**Figure 3.** DBD persistence on atomic lines 585.25 (1), 344.77 (2), 576.44 nm (3) and ion lines 333.48 (4), 439.20 nm (5).  $P_{\text{Ne}} = 1.35$  Torr.

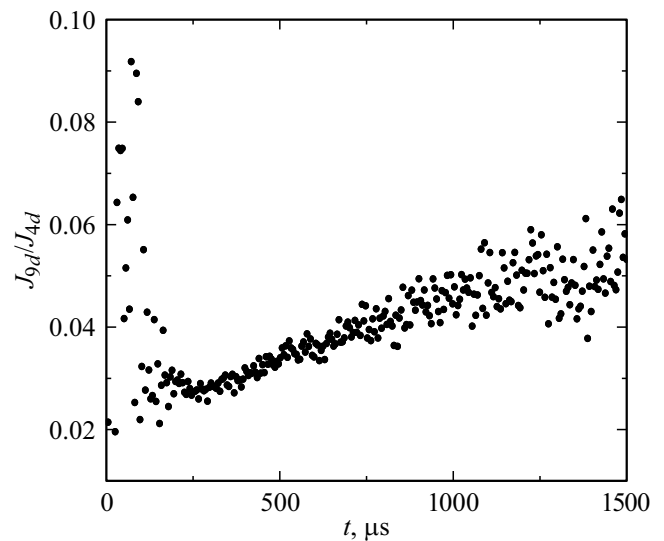


**Figure 4.** The ratio of the intensities of the lines 439.35 (9d → 3p) and 576.44 nm (4d → 3p).

of atomic lines for levels with principal quantum numbers  $n = 4$  (576.44 nm),  $n = 5$  (503.77 nm,  $\varepsilon^* = 0.55$  eV),  $n = 6$  (line 464.54 nm,  $\varepsilon^* = 0.28$  eV),  $n = 7$  (457.51 nm,  $\varepsilon^* = 0.275$  eV), and only the fluxes of quanta from the 8d and 9d levels changed noticeably differently in the afterglow. This difference is demonstrated in Fig. 4. With regard to the ion spectrum, it is enough to note the identical behavior of the 333.48 and 439.20 nm lines with a difference in the bond energy of their upper levels of more than 6 eV.

## 2. Determination of relative recombination rates

The key point of the proposed algorithm is as follows. Based on the strong dependence of the coefficients  $\alpha_{1cr}(T_e)$  and  $\alpha_{2cr}(T_e)$  on the electron temperature, we will try to predict the response of the intensities of atomic and ion lines to pulsed heating of electrons in the afterglow. Obviously, for some time we will exclude the recombination mechanism from the kinetics of the ion densities  $\text{Ne}^+$  and  $\text{Ne}^{++}$ . For example, by increasing the temperature by only twice, we reduce the rates of processes (1) and (2) by more than 20 times. Meanwhile, the accompanying mechanism of ambipolar diffusion, the rate of which is proportional to the electron temperature, practically does not add diffusion losses, which for a neon pressure of 1.7 Torr in the experiment discussed below follows from simple estimates of the rate of the process based on known data [14,16] on mobility ions  $\text{Ne}^+$  and  $\text{Ne}^{++}$ . In this case, we can expect that the ion densities  $[\text{Ne}_{\text{RF}}^+]$  and  $[\text{Ne}_{\text{RF}}^{++}]$  in the plasma after heating by a radio frequency (RF) field, and therefore the intensity  $J^{\text{RF}}$ , should be higher than without heating (here the index RF denotes the presence of a pulsed radio frequency plasma heating). Moreover, these changes will be proportional exclusively to the rate constants  $\alpha_{1cr}$  and  $\alpha_{2cr}$  in plasma without heating, since the rates of all other processes involving these plasma particles have not changed. We verified these assumptions by calculations as part of the model [2], which allows to describe quite well the evolution of the intensities of the lines of the atomic spectrum in the afterglow. The modeling results are shown in Fig. 5. Electron heating was simulated by adding a heat source of duration  $1 \mu\text{s}$  to the equation for  $T_e(t)$ . Its power was selected in such a way that the  $J_a(t)$  stroke was close to that observed in the experiment on the 576.44 nm line. The dependence of the coefficient CRR (1) on temperature and electron density was given by formula (6). It can be seen that the model solution corresponds to expectations and, in particular, confirms the opportunity, in a first approximation, of neglecting the role of ambipolar diffusion in the kinetics of ions  $\text{Ne}^+$ . This is indicated by the proximity of solutions at times  $t > t_m$  beyond the maximum  $J_a(t)$  after electron heating in the full model (curve 2) and with the suppression of temperature growth in the term of the equation for density  $[\text{Ne}^+]$ , which describes the dependence of the diffusion constant on  $T_e$  (curve 3). Finally, simulating the elimination of collisional radiative recombination in the model during the increase in  $T_e$  by simply „turning“ off the corresponding term in the equation for  $[\text{Ne}^+]$  for this time (curve 4) is in good agreement with the heating effect at  $t > t_m$ .

The results of the experiment are presented in Fig. 6, the data of which demonstrate the effect in the atomic and ion spectra. The electrons were heated by a weak radio frequency field with pulses of duration  $1 \mu\text{s}$ . It can be seen that, as one would expect, the response of the ion line to heating turns out to be somewhat stronger than the

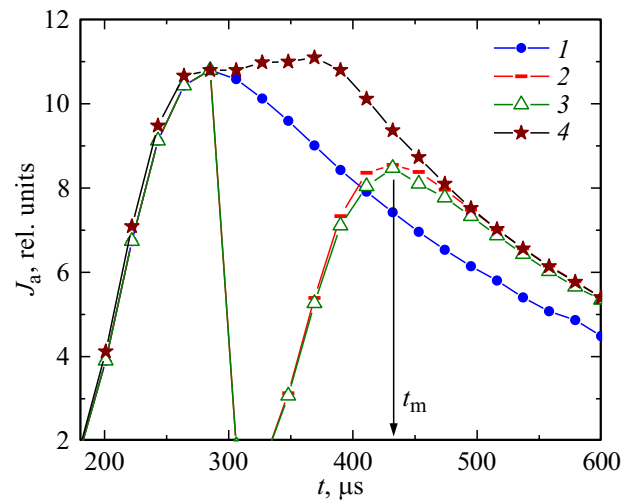


**Figure 5.** Simulating the intensity of an atomic line in the afterglow:  $t = 0$  corresponds to the beginning of the afterglow,  $P_{\text{Ne}} = 1.7 \text{ Torr}$ ,  $[e](t = 0) \approx 1.3 \cdot 10^{11} \text{ cm}^{-3}$ , (1,4) without electron heating, (2,3) with electron heating, (3) with suppression of ambipolar diffusion during heating, (4) with suppression of CRR ions during heating  $\text{Ne}^+$ .

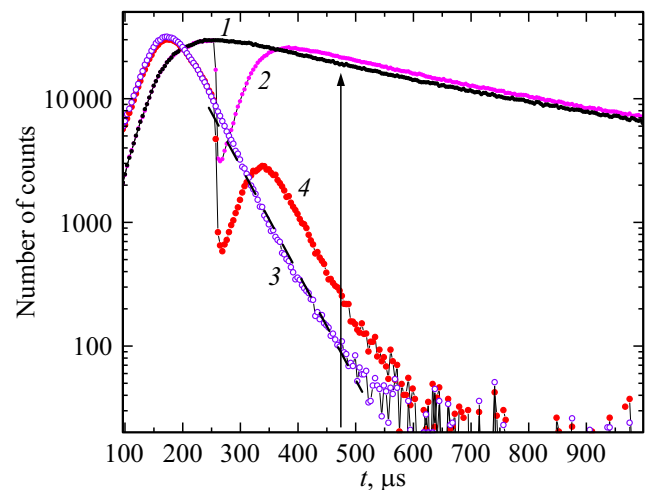


**Figure 6.** Afterglow without heating plasma electrons (1,3) and with pulsed heating of plasma electrons (2,4), (1,2) line 576.44 nm, (3,4) ionic line 333.48 nm. Dashed line — approximation by exponential dependence.

576.44 nm line emitted by the  $4d$  level of the neon atom, as follows from (6): at an electron density  $[e] \approx 10^{11} \text{ cm}^{-3}$  the dependence  $\alpha_{1cr}(T_e)$ , although not much differs from  $T_e^{-4.5}$ .

We will assess the  $\alpha_{2cr}/\alpha_{1cr}$  ratio based on experimental data as part of the following assumptions.

a) The intensities of spectral lines in the stage of plasma decay are proportional to the recombination fluxes, i.e. equalities (3), (4) are satisfied.

b) For ion densities it is fair

$$[\text{Ne}^{++}] \ll [\text{Ne}^+]. \quad (8)$$

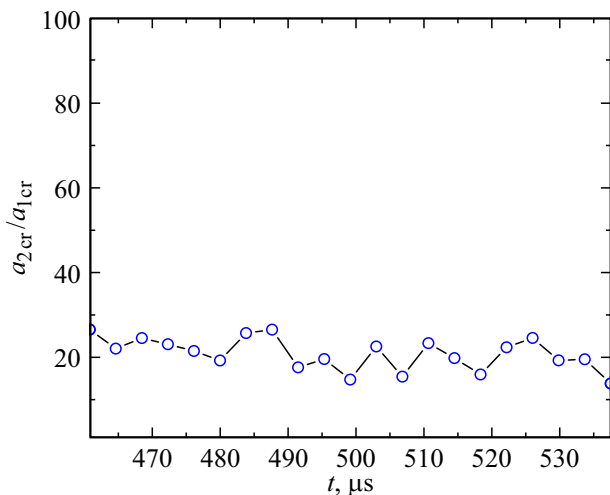


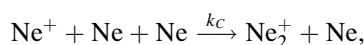
**Figure 7.** Ratios of recombination coefficients according to formula (11).

c) The density of molecular ions is also low:

$$[\text{Ne}_2^+] \ll [\text{Ne}^+]. \quad (9)$$

Then  $[\text{Ne}^+] \approx [e]$ .

For satisfiability (8), the experiment under discussion was performed at a noticeably higher pressure  $P_{\text{Ne}} = 1.7$  Torr (to the detriment to the brightness of ion lines) than in [1–3]. This minimizes the influence of conversion (7) on the course of the intensities of the  $J_a(t)$  lines in the experiment with electron heating, and, importantly, reduces the role of ambipolar diffusion in the kinetics of ions during the heating time. Inequality (9) follows from assessments of the rates of known [8] processes of destruction and formation of molecular ions, the main of which is conversion in triple collisions:



$k_c \sim 5 \cdot 10^{-32} \text{ cm}^6 \text{ s}^{-1}$ , is ineffective at such low pressures.

Let us compare the intensities of the atomic and ion lines in the afterglow with and without heating of electrons at the moment of time (shown by a vertical arrow) when the relaxation of the intensity of the 576.44 nm line to a new quasi-steady-state value has completed. Due to the exclusion of recombination for a time  $\Delta t$  (approximately  $100 \mu\text{s}$ , Fig. 6), the ion density  $[\text{Ne}^+]$  in the afterglow with electron heating will be higher by the amount

$$\Delta[\text{Ne}^+] \sim \Delta[e] = \alpha_{1cr}[e]^3 \Delta t.$$

Then

$$\begin{aligned} J_a^{\text{RF}}/J_a &= ([e] + \Delta[e])^3/[e]^3 \approx 1 + 3\Delta[e]/[e], \\ J_a^{\text{RF}}/J_a - 1 &= \alpha_{1cr}[e]^2 \Delta t * 3, \end{aligned} \quad (10)$$

as  $\Delta[e]/[e] \ll 1$ , which follows from the insignificant effect of electron heating on the quasi-steady-state intensity  $J_a$  at  $t > t_m$ .

To calculate the ratio  $J_i^{\text{RF}}/J_i$ , we take into account that the change in density  $[\text{Ne}^{++}]$  at  $t > t_1$  in a plasma without electron heating has a character close to exponential, i.e. occurs at a practically unchanged electron density (Fig. 6). Then the number of ions in this plasma and, consequently, the intensity  $J_i$  compared to the afterglow with recombination turned off will differ by the coefficient  $\exp\{-\alpha_{2cr}[e]^2 \Delta t\}$ :

$$J_i \sim J_i^{\text{RF}} \exp\{-\alpha_{2cr}[e]^2 \Delta t\}.$$

Therefore,

$$\ln(J_i^{\text{RF}}/J_i) \sim \alpha_{2cr}[e]^2 \Delta t,$$

whence, taking into account (10) we have

$$\alpha_{2cr}/\alpha_{1cr} = \ln(J_i^{\text{RF}}/J_i)3/(J_i^{\text{RF}}/J_i - 1). \quad (11)$$

We tested this algorithm on the brightest ion lines in the afterglow, 439.20 and 333.48 nm. The course of the latter, together with the 576.44 nm line, is shown in Fig. 6. The response of the intensity of the 439.20 nm line to electron heating was identical to the reaction of the 333.48 nm line. Data processing based on (11) with averaging of intensities over three time channels of a photon counter (measurements of intensities in Fig. 6 were carried out with a resolution of  $1.28 \mu\text{s}$ , in the graph they are presented as the result of averaging over three channels) for the ratio of coefficients gave the result presented in Fig. 7. It can be seen that the ratio of the recombination coefficients does not depend much on the choice of the moment of time for comparing the intensity ratio, provided that by this time (vertical arrow in Fig. 6) the system forgets about the perturbation introduced by pulsed heating. Averaging the data in Fig. 7 within the specified time period, we find  $\alpha_{2cr}/\alpha_{1cr} = 21 \pm 4$ . A similar procedure using the 439.20 nm ion line gives a similar ratio of recombination

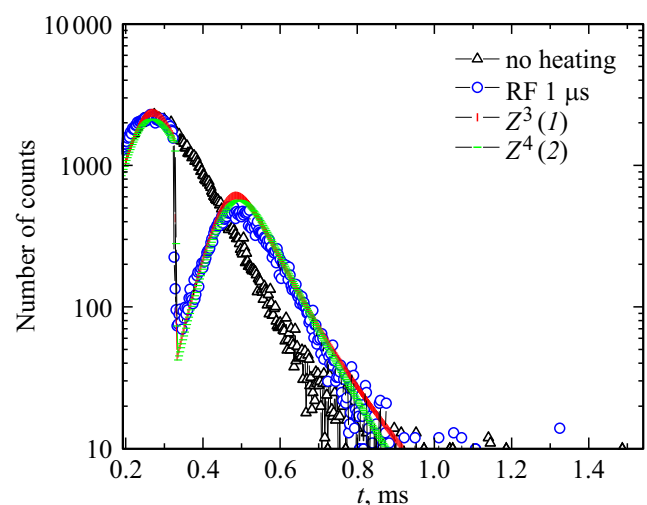


**Figure 8.** Experimental data and model solutions for ionic lines. The values of the ratio of recombination coefficients are 8 (1) and 18 (2).

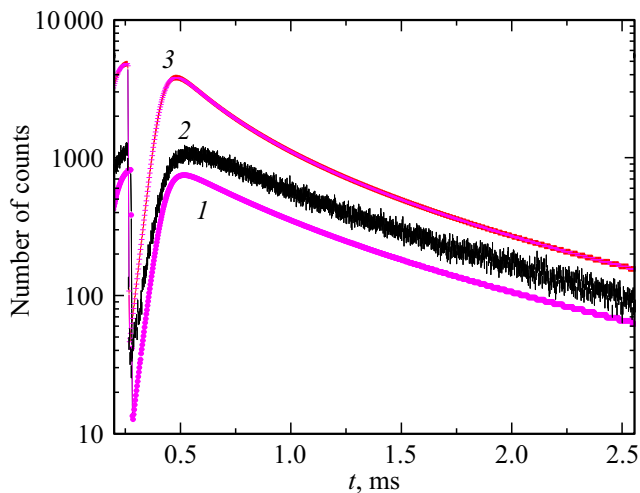


**Figure 9.** Experimental data (2) and model solutions for the values of the ratio of recombination coefficients 18 (1) and 8 (3). Conditions are the same as in Fig. 8. The curves 1 and 3 are shifted relative to 2 for ease of reading.

coefficients, but with a larger error due to the noticeably lower intensity of the line.

The obtained result indicates an even greater difference in the recombination rates of singly and doubly charged ions than was found in [3] based on a comparison of the dependence  $J_i(t)$  with the model solution corresponding to  $\alpha_{2cr}/\alpha_{1cr} \sim Z^4$  in formula (5). Let us recall that to simulate the behavior of ion lines [3] we used model parameters (i.e., a set of process rate constants taken into account in the system of differential equations), which provide the best description of the evolution of  $J_a(t)$  atomic lines in a decaying plasma, and with these parameters, in particular, the ratio  $\alpha_{2cr}/\alpha_{1cr}$  was selected for the best description  $J_i(t)$ . As follows from the data presented in [3], it was not possible to construct an equally adequate description of the evolution of the intensities of ion lines. In this regard, the question arises, which data best reflects the actual ratio of the sought constants. In terms of assessing the uniqueness of the conclusions obtained based on modeling, we give the following example (Fig. 8, 9). Figure 8 shows the opportunity of constructing model solutions corresponding to experimental data for the ion line in both cases:  $\alpha_{2cr}/\alpha_{1cr} = 8$  and  $\alpha_{2cr}/\alpha_{1cr} = 18$ . For  $\alpha_{2cr}/\alpha_{1cr} = 18$ , the simulation of  $J_i(t)$  uses plasma parameters that give an almost ideal description of  $J_a(t)$  (Fig. 9), increasing the initial electron density  $[e](t=0)$  by 1.7 times, but maintaining the characteristic cooling time of electrons due to electron-ion collisions and selecting constant  $k_c$  of the ion conversion process  $\text{Ne}^{++}$  within the values proposed in [14,15]. This replacement, in our opinion, does not go beyond reason, since the frequency of electron-ion collisions, as is known, is calculated using approximate formulas, and the electron density is determined in our experiment with an error of  $\approx 30\%$  [1]. So the main argument in favor of choosing  $\alpha_{2cr}/\alpha_{1cr} = 18$  based on

simulation is the consistency of the solution for  $J_a(t)$  with experiment, which, as Fig. 9 shows, is lost in the opposite case. In this regard, we consider the result of this work, firstly, as confirmation of the adequacy of the afterglow model [2,3], and, secondly, as a demonstration of the possibility of estimating the rate of collisional-radiative recombination of doubly charged ions directly on the basis of experimental data using fairly obvious assumptions. It is important that this approach eliminates the uncertainty in the available data on the conversion rate of  $\text{Ne}^{++} \rightarrow 2\text{Ne}^+$  ions in collisions with neon atoms.

## Conclusion

In this work, a direct estimation of the ratio of the coefficients of collisional-radiative recombination of ions  $\text{Ne}^{++}$  and  $\text{Ne}^+$  with electrons was obtained based on the results of spectroscopic observations of the evolution of the intensities of atomic and ion lines in the afterglow of a low-pressure dielectric barrier discharge. As an initial premise, we used the obvious opportunity of suppressing the processes of collisional-radiative recombination of both ions by „heating“ electrons for a short time in the plasma decay stage, followed by an analysis of the differences in the reactions of the spectral lines of the atomic and ion spectra. The obtained result significantly exceeds both the predictions of the collisional model of the process and the results of numerical calculations based on the analysis of the solution of the system of equations for the populations of excited levels of the atom and ion in the quasi-steady-state approximation.

## Conflict of interest

The authors declare that they have no conflict of interest.

## References

- [1] V.A. Ivanov. Plasma Sources Sci. Technol., **29**, 045022 (2020). DOI:10.1088/1361-6595/ab7f4c
- [2] V.A. Ivanov. Opt. i spektr., **129** (8), 992 (2021) (in Russian). DOI: 10.61011/EOS.2023.11.58042.5370-23 [V.A. Ivanov. Opt. Spectrosc., **129** (10), 1104 (2021). DOI: 10.1134/S0030400X21080099].
- [3] V.A. Ivanov. Opt. i spektr., **130** (7), 1004 (2022) (in Russian). DOI: 10.61011/EOS.2023.11.58042.5370-23 [V.A. Ivanov. Opt. Spectrosc., **130**(7), 806 (2022). DOI: 10.61011/EOS.2023.11.58042.5370-23].
- [4] A.V. Gurevich, L.P. Pitaevskii. Sov. Phys. JETP, **19** (4), 870 (1964).
- [5] D.R. Bates, A.E. Kingston, R.W.P. McWhirter. Proc. Roy. Soc. London, **267**, 297 (1962).
- [6] J.J. Thomson. Phil. Mag., **47**, 337 (1924). DOI: 10.1080/14786442408634372
- [7] L.M. Biberman, V.S. Vorob'yev, I.T. Yakubov. Kinetika neravnovesnoy nizkotemperaturnoy plazmy (Nauka, M., 1982) (in Russian).

- [8] B.M. Smirnov. *Iony i vozbuždennyye atomy v plazme* (Atomizdat, M., 1974) (in Russian).
- [9] J. Stevefelt, J. Boulmer, J.-F. Delpeche. *Phys. Rev. A*, **12**, 1246 (1975).
- [10] H.A. Bethe, E.E. Salpeter. *Quantum Mechanism of One- and Two-Electron Atoms* (Academic Press, NY., 1957).
- [11] P. Mansbach, J. Keck. *Phys. Rev.*, **181**, 275 (1969).
- [12] S.V. Gordeev, V.A. Ivanov, Yu.E. Skoblo. *Opt. Spectrosc.*, **127**, 418 (2019). DOI: 10.1134/S0030400X19090133.
- [13] Y.J. Shiu, M.A. Biondi, D.P. Sipler. *Phys. Rev. A*, **15**, 494 (1977).
- [14] F.J. de Hoog, H.J. Oskam. *J. Appl. Phys.*, **44**, 3496 (1973).
- [15] R. Johnsen, M.A. Biondi. *Phys. Rev. A*, **18**, 996 (1978).
- [16] R. Johnsen, M. A. Biondi. *Phys. Rev. A*, **18**, 989 (1978).

*Translated by E.Potapova*